Supplementary Materials

This supplement contains more detailed descriptions of all methods and supplementary figures 1 and 2.

Methods

Animal strains and husbandry

All animal experiments were carried out according to the guidelines of the Association for Research in Vision and Ophthalmology (ARVO) and were approved by the Institutional Animal Care and Use Committee at the Schepens Eye Research Institute. We used a cross between C57bl/6 and hGFAPpr-GFP mice. The latter express GFP in individual astrocytes in the optic nerve and other parts of the CNS [1-3]. The original hGFAPpr-GFP strain was created on the FVB/N genetic background and develops retinal degeneration [1]. We crossed the mutation into the C57bl/6 background to eliminate the *rd*1 mutation in the original strain. All animals were also tested for the absence of retinal degeneration by optical coherence tomography (OCT). GFP expression was verified by inspecting an ear punch under a fluorescent microscope because in this strain, peripheral glial cells are also labeled and can be observed directly. Male and female mice of 2-8 months were used for all experiments.

Optical coherence tomography (OCT)

In vivo posterior segment images were obtained using an ultrahigh-resolution SD-OCT system (Bioptigen, Morrisville, NC) before, and one month after microbead injection. Mice were anesthetized by intraperitoneal injection of ketamine (100 mg/kg) and xylazine (12 mg/kg), followed by local anesthesia with proparacaine hydrochloride (0.5%; Bausch& Lomb, Tampa, FL). Both averaged single B scan and volume scans were obtained with images centered on optic nerve head.

Microbead injection

Chronic intraocular hypertension was induced by the injection of microbeads (15µm diameter, Invitrogen, Carlsbad, CA) into the anterior chamber of the right eye, essentially as described by the developers of the method [4-6]. Mice were anesthetized and a small corneal incision was made in the paracentral area with a 30 gauge needle. A glass micropipette attached to a Hamilton syringe was inserted through the puncture hole to create an air bubble in the anterior chamber. The micropipette was removed, loaded with microbeads, and reinserted into the anterior chamber taking care to avoid the lens. A total of 2-3 µl of microbeads (2.7×10^7 beads in sterile saline solution) were injected into the right eye. The air bubble serves to prevent a loss of microbeads when the needle is withdrawn, and it is completely absorbed within days after the procedure. Antibiotic ointment was applied after the surgery. All the contralateral uninjected eyes were considered as controls. Another group of mice was injected unilaterally with 2-3 µl PBS as an additional control.

IOP measurement

Intraocular pressure (IOP) was measured non-invasively in both eyes in every group one time before and twice weekly after microbead or PBS injection. All measurements were taken at the same time in the morning to minimize circadian variation in IOP. Mice were anesthetized with isoflurane inhalation (2%–4%; Webster Veterinary, Sterling, MA) that was delivered via a nosecone. IOP was measured using a rebound tonometer (TonoLab; Colonial Medical Supply, Espoo, Finland) within 2 minutes after the onset of anesthesia, which was defined as absence of movement and eye blinking, and smooth breathing. Each recorded IOP was the average of five mean values which were obtained from the tonometer by measuring one eye six times to get each mean value. The cumulative IOP (cIOP) was calculated for each eye as the area under the curve of IOP over time with a user-written Matlab routine.

Tissue preparation and embedding

To avoid structural damage while obtaining the eye with the optic nerve, the skull was opened and the brain was carefully removed to expose the underlying optic nerve and chiasm [3, 7]. The head with the eyes and optic nerves in situ were fixed for 2 h in 4% paraformaldehyde and washed with PBS. The orbital bones and retrobulbar tissue were removed to isolate the eyeball with the optic nerve attached. The dura surrounding the optic nerve was delicately removed [3, 7]. Then the cornea was cut off along the limbus, the lens and vitreous were removed, and the sclera and pigment epithelium were peeled away from the neural retina. Finally, the optic nerve was gently detached from the retina, embedded in 6% agarose, and sectioned at 100 µm (for confocal imaging), or 200 µm (for later electron microscopy) thickness in transverse orientation using a vibratome (Leica VT1000 S). For retinal ganglion cell counting, four small radial incisions were made in the retina, so that the retina could be flat-mounted ganglion side up on AA nitrocellulose filters (MF19 Millipore, Billerica, MA).

Confocal microscopy and image reconstruction

Images of astrocytes located in the unmyelinated segment of the optic nerve were obtained on a Leica TCS SP8 confocal microscope system (Leica Microsystems, Buffalo Grove, IL) using a 63X glycerol immersion objective. Individual agarose sections were kept in order starting from 1 (at the level of the sclera to 100 µm behind the sclera) to 4 (400-500 µm behind the sclera). Sections beyond that were in the myelinated portion of the optic nerve. We restricted the analysis to the glial lamina, and astrocytes in the optic nerve proper (myelinated portion) were not imaged. Image stacks were taken through the whole extent of the cell. Image size was 1024x1024 pixels in x/y, corresponding to a resolution of 0.1805 µm per pixel. The z step size was 0.33 µm. The 3D reconstruction of astrocytes was accomplished using a volume visualization program (Amira, Visage Imaging, San Diego, CA).

Transmission electron microscopy

After confocal microscopy the vibratome optic nerve sections with the surrounding agarose were immediately immersion fixed with half strength Karnovsky's fixative for 2 h at room temperature. After fixation, samples were rinsed with 0.1M sodium cacodylate buffer, post-fixed with 2% osmium tetroxide in 0.1M sodium cacodylate buffer for 1.5 hours, rinsed in deionized water, then *en bloc* stained with 2% aqueous uranyl acetate for 30 minutes. Samples were dehydrated with graded ethyl alcohol solutions, transitioned with propylene oxide and resin infiltrated in tEPON-812 epoxy resin (Tousimis, Rockville, Maryland.) in a lynx II EM Tissue Processor (Electron Microscopy Sciences, Hatfield, PA). Processed tissues were oriented in tEPON-812 epoxy resin and polymerized in silicone molds using an oven set for 60^{o}C for 2 days. Semi-thin cross-sections for light microscopy were cut at 1-micron and stained with 1% toluidine blue in 1% sodium tetraborate aqueous solution on a slide warmer for assessment and screening regions of the tissue block face for ultra-thin sectioning. Ultra-thin sections (70-90 nm) were cut from the epoxy block using a Leica EM UC7 ultramicrotome (Leica Microsystems, Buffalo Grove, IL) and a diamond knife, collected and air-dried onto uncoated 200 mesh grids and 2x1mm single slot formvar/carbon coated grids using the 'Perfect loop' tool (Electron Microscopy Sciences, Hatfield, Pennsylvania.) Grids were stained with aqueous 25% uranyl acetate replacement (Electron Microscopy Sciences, Hatfield, Pennsylvania) for 30 minutes, rinsed in five changes of deionized water then Sato's Lead citrate for 5 minutes, and rinsed in six changes of deionized water and dried using the Hiraoka grid staining technique. Stained grids were imaged using a FEI Tecnai G2 Spirit transmission electron microscope (FEI, Hillsboro, Oregon) at 8o kV interfaced with an AMT XR41 digital CCD camera (Advanced Microscopy Techniques, Woburn, Massachusetts) for digital TIFF file image acquisition.

Immunohistochemistry

The whole-mounted retinas were incubated in blocking solution (5% donkey serum, 0.3% Triton X-100) for 1 hour at room temperature, and incubated in primary antibodies for 3-4 days at 4°C. The primary antibodies used were: rabbit anti-β-III tubulin (1:200, Cell Signaling), mouse anti-Brn3a (1:200, Chemicon). Afterward, retinas were washed in PBS (3×10 min) and incubated in secondary antibodies conjugated with FITC (1:400, donkey anti rabbit IgG, Jackson Immunoresearch), rhodamine (1:400, donkey anti mouse IgG ,Jackson Immunoresearch), for 3 days at 4°C. Subsequently, retinas were counterstained with the nuclear dye DAPI (Life technologies, Grand Island, NY), and mounted in Vectashield (Vector Laboratories, Burlingame, CA).

Ganglion cell counting

Retinal ganglion cells (RGCs) were counted on whole-mounted retinas after immunostaining for Brn3a and β-III tubulin. The images were acquired with a 63X glycerol immersion objective on a Leica TCS SP8 confocal microscope system. The retina was divided into quadrants and two mid-peripheral regions (defined as equidistant to the site of optic nerve head and the border of the retina) were imaged in every quadrant (8 regions of 184.52 µm by 184.52 µm per retina). To include all cells in the ganglion cell layers, z-stacks were taken through the ganglion cell layer at a step size of 0.5 µm, and maximum-intensity projections of these stacks were made in ImageJ. All cells in the ganglion cell layer that co-localized with both anti-β-III tubulin and anti-Brn 3a were counted and the ganglion cell density per retina was calculated. Cells positive for β-III tubulin were counted manually by individuals blinded to different groups of the animal ImageJ (National Institute of Health, USA), Brn3a-positive cells were counted semi-automatically in a user-written Matlab routine (version R2013b, The Mathwork Inc. Natick, Massachusetts, USA). Differences in ganglion cell counts were tested for significance using Student's t test.

Cell tracing

Every animal received a number code after the experiment and the investigator performing morphometric measurements and statistical analysis was ignorant of the IOP history of the eye. Unprocessed confocal image stacks through the glial lamina were imported to ImageJ. To quantify longitudinal processes individual astrocytes were traced using the Simple Neurite Tracer plugin [8]. Image stacks containing more than 10 labeled cells were not analyzed because in these cases it was impossible to discern individual cells. For examples of digitized astrocytes, see Supplementary Figure 1. The length of all processes was measured for each cell and the ratio of longitudinal process length to total process length (L/T) was calculated. Differences between groups were tested for significance using a Wilcoxon rank sum test. All statistical tests were done in Matlab.

Data sharing

All original unprocessed images and image stacks were deposited in the Harvard Dataverse and are accessible under https://dataverse.harvard.edu/dataverse/Astrocytes_Glaucoma .

References

1. Nolte C, Matyash M, Pivneva T, et al. GFAP promoter-controlled EGFP-expressing transgenic mice: a tool to visualize astrocytes and astrogliosis in living brain tissue. *Glia* 2001;33:72-86.
2. Emsley JG, Macklis JD. Astroglial heterogeneity closely reflects the neuronal-defined anatomy of the adult murine CNS. *Neuron Glia Biol* 2006;2:175-186.
3. Sun D, Lye-Barthel M, Masland RH, Jakobs TC. The morphology and spatial arrangement of astrocytes in the optic nerve head of the mouse. *J Comp Neurol* 2009;516:1-19.
4. Sappington RM, Carlson BJ, Crish SD, Calkins DJ. The microbead occlusion model: a paradigm for induced ocular hypertension in rats and mice. *Invest Ophthalmol Vis Sci* 2010;51:207-216.
5. Crish SD, Sappington RM, Inman DM, Horner PJ, Calkins DJ. Distal axonopathy with structural persistence in glaucomatous neurodegeneration. *Proc Natl Acad Sci U S A* 2010;107:5196-5201.
6. Chen H, Wei X, Cho KS, et al. Optic neuropathy due to microbead-induced elevated intraocular pressure in the mouse. *Invest Ophthalmol Vis Sci* 2011;52:36-44.
7. Sun D, Qu J, Jakobs TC. Reversible reactivity by optic nerve astrocytes. *Glia* 2013;61:1218-1235.

8. Longair MH, Baker DA, Armstrong JD. Simple Neurite Tracer: open source software for reconstruction, visualization and analysis of neuronal processes. *Bioinformatics* 2011;27:2453-2454.

Supplementary Figures

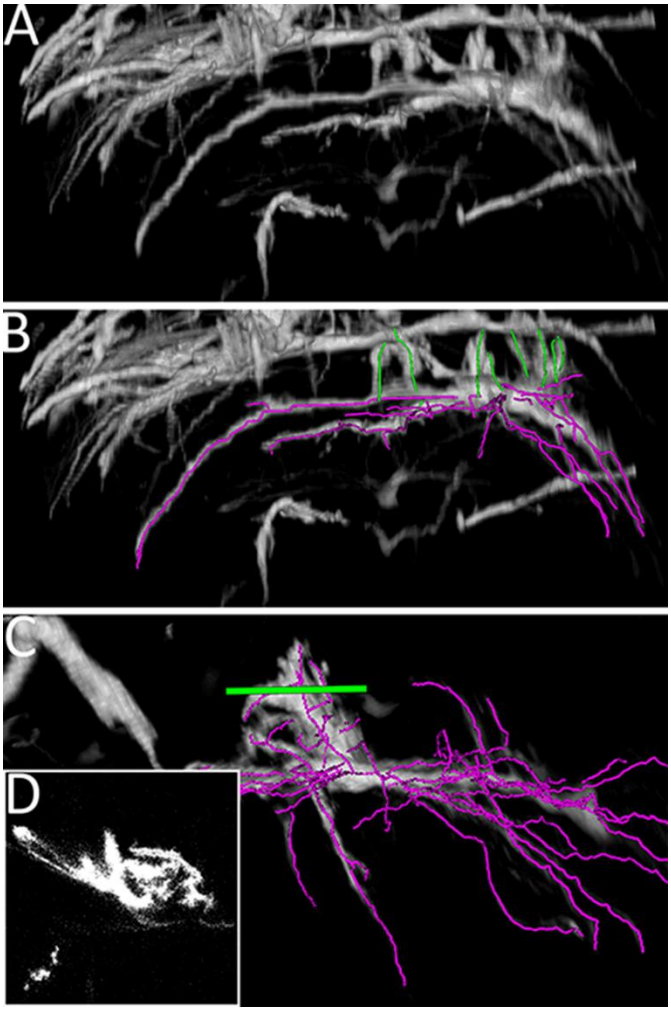

Figure S1. Digital representations of optic nerve head astrocytes. **A, B:** Volume rendering of an astrocyte in the glial lamina before (A) and after (B) tracing with Simple Neurite Tracer. The regular processes of this astrocyte are indicated in magenta to highlight the concave shape of the cell. Longitudinal processes (indicated in green) are extending from the regular processes in the direction of the myelination transition zone. **C, D:** Astrocyte with a complex longitudinal process. C shows the tracing and the insert D show a cross-section of the longitudinal process at the level indicated by a green bar in C.

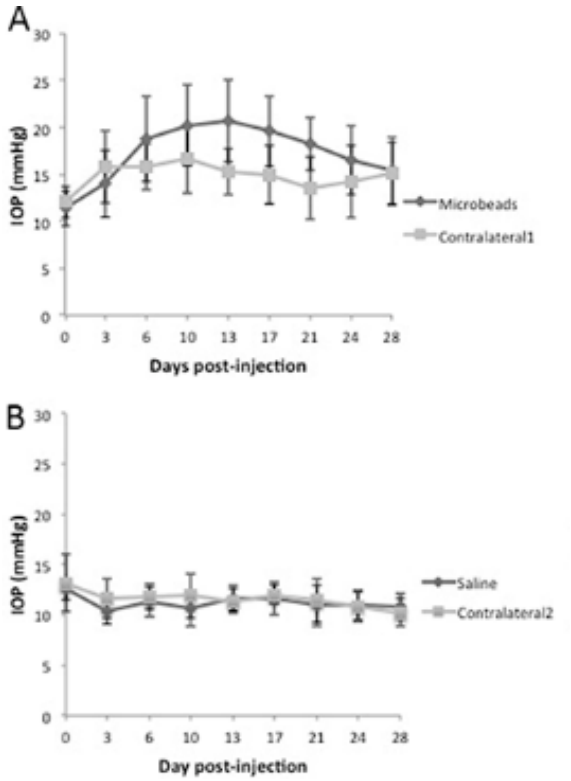

Figure S2. Induction of ocular hypertension with the microbead occlusion model. **A:** The IOP in the microbead-injected eyes (dark line) and their contralateral eyes (gray line). **B:** The IOP in the saline-injected eyes (dark line) and their contralateral eyes (gray line). Data are presented as mean ± SD. n = 23 (A), n = 8 (B). IOP= intraocular pressure.